Trapping model for the non-Arrhenius ionic conductivity in fast ion-conducting glasses

2003 J. Phys.: Condens. Matter 15 S1643

(http://iopscience.iop.org/0953-8984/15/16/312)

INSTITUTE OF PHYSICS PUBLISHING JOURNAL OF PHYSICS: CONDENSED MATTER

J. Phys.: Condens. Matter **15** (2003) S1643–S1658 PII: S0953-8984(03)60970-7

Trapping model for the non-Arrhenius ionic conductivity in fast ion-conducting glasses*

S W Martin[1], D M Martin, J Schrooten and B M Meyer

Department of Materials Science and Engineering, Iowa State University of Science and Technology, Ames, IA 50011, USA

Received 18 March 2003
Published 14 April 2003
Online at stacks.iop.org/JPhysCM/15/S1643

Abstract

A new model is proposed to describe the non-Arrhenius conductivity observed in a series of optimized fast ion-conducting silver thioborosilicate glasses. Its essential feature is that the mobile cations are thought to conduct from one open site to the next open available site and, in this process, naturally by-pass filled or unavailable sites. The thermal excitation of cations out of their equilibrium sites is taken to be the mechanism for generating the open and available anion sites. Hence, the mean free path for a drifting cation between open available sites is directly proportional to the activated carrier concentration and is therefore a strong function of temperature. There is also a weak temperature dependence for the mean free path that arises because the capture cross section for a drifting cation by a stationary anion trap varies with drift velocity, e.g. the momentum of a fast cation allows it to closely approach an anion trap while avoiding capture or back scattering. The capture cross section of a cation by an anion trap is large because the interaction is electrostatic rather than geometric in origin. The model is shown to be in good agreement with all of our experimental data for silver thioborosilicate glasses and all model parameters are physically defined and reasonable in value. The model predicts a simple high-temperature conductivity dependence that is not exponential in nature. The model is also proposed to be valid for other materials such as crystalline conductors.

(Some figures in this article are in colour only in the electronic version)

1. Introduction

Ion-conducting glasses are of high interest due to their potential use as solid electrolytes in battery applications where they have several advantages over their crystalline counterparts. For example, they have an isotropic conductivity and an absence of grain boundaries and their

* Proceedings of the CECAM Workshop on 'Atomic Structure and Transport in Glassy Networks'.

[1] Author to whom any correspondence should be addressed.

0953-8984/03/161643+16$30.00

wide compositional flexibility allows for the optimization of electrolyte properties. Glasses can also be fabricated into complex shapes such as thin films and very small batteries made using ion-conducting thin film glasses; these should enable new applications in microelectronics. Comprehensive studies of the variation of the ionic conductivity with temperature, composition and structure are the key to understanding transport phenomena in glasses [1–11].

Recently, Kincs and Martin [12] reported the discovery of fast ion-conducting (FIC) glasses in the AgI–Ag_2S–B_2S_3–SiS_2 (silver thioborosilicate) system. This complex system was specifically chosen by using known relationships for the composition dependence of the ionic conductivity in an effort to develop the highest ionically conducting glass to date. As a result, the glasses produced in this system have exhibited record high room-temperature ionic conductivities as well as good chemical stability, a known challenge for chalcogenide systems. More recently, Schrooten has re-examined this series of glasses by measuring the conductivity to higher temperatures and carefully inspecting them for phase separation and crystallization [13].

While ionic conductivities as high as $10^{-2}(\Omega\,\mathrm{cm})^{-1}$ at room temperature have been measured in the silver thioborosilicate system, a strong non-Arrhenius temperature dependence decreases the conductivity to several orders of magnitude lower than that expected from the observed Arrhenius behaviour at low temperatures (LTs). This behaviour is not exclusive to the silver thioborosilicate system: it has also been observed in, for example, glassy $Ag_7I_4AsO_4$ [14].

Several researchers have postulated explanations for this non-Arrhenius behaviour. Maass *et al* [15] believe that it arises as the result of Coulombic interactions between the silver ions at higher temperatures. Ngai and Rizos [16] have used their coupling model to interpret the data and suggest that the observed behaviour is indicative of an upper limit for the ionic conductivity in a glass. While accurately describing the non-Arrhenius behaviour of the conductivity, these models have yet to provide a physical picture of its root cause.

This paper proposes a new model wherein the non-Arrhenius behaviour is caused by frequent mobile cation trapping events that result from a rapidly increasing number of 'open' anion sites in the glass with increasing temperature. At LTs, open sites are less numerous due to the low thermal probability of creating activated cations which therefore conduct from site to site over relatively large distances. At higher temperatures, and in the range of the non-Arrhenius temperature dependence, the fraction of open sites increases, along with an equal fraction of mobile cations, and thermally activated carriers are more likely to find a nearby trap. It is believed that this higher efficiency of cation trapping at elevated temperatures leads to the non-Arrhenius ionic conductivity.

2. Model development

2.1. Background

Mobile cations in compositionally optimized glasses, such as those being examined here, are considered to conduct from site to site by the well-known thermally activated hopping mechanism [17]. The cation sites are assumed to be characterized by bond distances, coordination numbers and overall site chemistry that vary from site to site. This creates a distribution of energy barriers, which is symmetric about a mean with a well-defined standard deviation, that governs the kinetics of the mobile cations [18]. The number of such cations available for conduction at any one temperature is likewise considered to be given by a summation over a well-known and accepted Boltzmann distribution of energy barriers.

In this way, the conduction process at LTs, $k_BT \ll \Delta E_{act}$, where ΔE_{act} is some average of the barrier distribution, is described by a relatively small number of thermally activated cations migrating with a relatively low drift velocity (determined by temperature) through a

disordered glassy network that has a relatively small number of 'open' anion sites, hereafter referred to as 'traps'. The conduction process must in this view be characterized as the cations exploring a significant fraction of the interstitial sites in the glass along their way towards finding a trapping site.

As the temperature is increased, the number of thermally activated mobile cations increases according to Boltzmann statistics. This likewise creates an increasing number of traps. Hence, at higher temperatures, the conduction process is characterized by greater numbers of mobile cations migrating with a higher drift velocity through the glass network where the traps are significantly greater in number and therefore closer together. In this view, the conductivity becomes a compromise between the number of activated carriers and the number of traps, the former working to increase and the latter working to decrease the conductivity. The non-Arrhenius conductivity then arises from the simple fact that, in the optimized glasses, these two competing effects are seen to the full. At LTs, the thermal activation of carriers is the dominant factor, thereby increasing the conductivity in an Arrhenius manner. At higher temperatures, the large number of traps has a dominant effect, thereby creating the non-Arrhenius conductivity.

In the following, a simple one-parameter model is developed that captures the essence of this description of the conduction process. The fundamentally important finding is that the carriers conduct for relatively large distances (tens of nanometres) between traps in these glasses, not because they are highly conducting FIC materials but rather because they are required to do so because the average barrier height relative to k_BT is sufficiently large ($T \sim 500$ K versus $\Delta E_{act}/k_B \sim 2000$ K) that even at high temperatures the number of mobile carriers is actually quite small (typically $\ll 1\%$). This forces, on average, the trapping sites to be relatively widely spaced. The trap separation is, nevertheless, strongly temperature dependent, decreasing with increasing temperature. This gives rise to a strongly temperature-dependent trapping of the mobile carriers which in turn leads to a strongly temperature-dependent conductivity. The conductivity exhibits a non-Arrhenius temperature dependence due to the temperature dependence of the trap separation and it appears to tend towards a maximum limiting value of $\sim 10^{-1}$–$10^{0}\ \Omega\ \mathrm{cm}^{-1}$.

2.2. Model

The dc conductivity, σ_{dc}, is taken to be the product of the mobile cation number density, $n(T)$, the mobile cation charge, $+e$, and the mobile cation mobility, $\mu(T)$ [7]

$$\sigma_{\mathrm{dc}} = n(T)e\mu(T). \tag{1}$$

The temperature-dependent number density of mobile cations is taken from the Boltzmann distribution

$$n(T) = n_{tot}\exp(-\Delta E_{act}/k_BT) \tag{2}$$

where n_{tot} is the total composition determined value and ΔE_{act} is the average activation energy for the conductivity. Below, we will expand equation (2) to include a distribution of such activation energies. The mobility is the ratio of the mean (thermal) drift velocity in the direction of the applied electrical field to the magnitude of the applied field

$$\mu(T) = v_x/(\partial V/\partial x). \tag{3}$$

The mean drift velocity of the mobile cations is determined as follows. First, a voltage gradient in the x direction causes the ions to drift in that direction with a mean free path length of λ between events that stop or alter their drift. The relationship of the cation's mean free path to the drift velocity is estimated from a balance between the thermal energy available to the cation and the additional energy supplied to the cation from the applied electric field. Hence,

$$m((v_{0x} + \Delta v_{max\,x})^2 + v_{0y}^2 + v_{0z}^2)/2 \cong mv_0^2/2 + mv_{0x}\Delta v_{max\,x} = k_BT + e\lambda\,\mathrm{d}V/\mathrm{d}x \tag{4}$$

where v_0, v_{0x} and $\Delta v_{\max\ x}$ are the initial (zero field) thermal velocity of the mobile cations, the initial (zero field) thermal velocity of the mobile cations in the x direction and the *maximum* change in the velocity of the mobile cations in the x direction due to the applied electrical field (taken to be along the x direction). Note that the mean drift velocity of the cation following application of the electrical field ($\overline{\Delta v_x} = v_x(T)$) will be the average of the change in velocity before the field is applied (zero) and the maximum change in velocity after the field is applied ($\Delta v_{max\ x}$) and equals $\Delta v_{max\ x}/2$. The approximation recognizes that the mean thermal velocity is much larger than the change in velocity due to the applied electrical field or, similarly, that the thermal energy is much larger than the potential energy created by the applied electrical field, 2500 J mol^{-1} versus 2.4×10^{-7} J mol^{-1}, respectively, at room temperature. v_{0x} and v_0 are related for isotropic motion by

$$v_0^2 = v_{0x}^2 + v_{0y}^2 + v_{0z}^2 = 3v_{0x}^2 \tag{5}$$

and the most probable thermal velocity in the absence of the electrical field is given by [19]

$$mv_0^2/2 = k_B T. \tag{6}$$

Finally, by combining equations (4)–(6) we have

$$v_x(T) = \overline{\Delta v_x} = \frac{1}{2} \frac{e\lambda}{\sqrt{2mk_BT/3}} \frac{\partial V}{\partial x} \tag{7}$$

which gives $\sim 4 \times 10^{-4}$ m s^{-1} for Ag^+ ions at room temperature for an average trap distance of 2 nm and a potential field of 0.05 V over a 1 mm thick sample. As expected this is much slower than the most probable thermal velocity of $\sim$200 m s^{-1} given by equation (6).

The trap distance is taken to be the parallel average of two trapping distances, λ_0 and λ_1. λ_0 is proposed to be a limiting 'frozen structure' trap distance that determines some intrinsic limiting value characteristic of the particular glass under study. λ_1 is the temperature-dependent trap distance created by the thermal excitation of cations from their equilibrium sites and, in this paper, we will assume two possible origins.

In scheme I, we will assume that the distance λ_1 arises because the open sites provide a 'geometric' trapping cross section for the mobile carriers. The hypothesis here is that the trapping site has a finite size, essentially that of the anion, e.g. a non-bridging oxygen in an oxide glass. A mobile cation in its random migration through the network will then have its trajectory altered or will eventually be stopped by this trapping anion. In this scheme we will use an ideal gas representation for the moving carriers.

In scheme II, we will assume that the trapping distance is electrostatic in origin, namely cation–anion Coulombic attraction, and will therefore use a more sensible ionic lattice plasma to model the behaviour of the mobile cations. Here, the hypothesis is that a cation migrating through the disordered network experiences the collective Coulombic interactions of all anions and cations in the glass and is therefore repelled if it approaches a cation and attracted if it approaches an anion. In the latter case, the Coulombic attraction can pull the cation into an anion trap where the effective trapping distance is strongly temperature dependent. At LTs, a cation will have a relatively low average thermal velocity and can be trapped at larger distances by an open anion site. At higher temperatures, and for the same anion and cation charges, the cation will have a higher thermal velocity and can only be trapped at shorter distances where the Coulomb field is largest: at larger distances the cation can effectively by-pass an anion trap because of its higher momentum.

In both of these schemes, the average trapping distance is taken to be the parallel average of the two trapping distances, namely

$$\frac{1}{\lambda(T)} = \frac{1}{\lambda_0} + \frac{1}{\lambda_1}. \tag{8}$$

In scheme I, where we use the ideal gas trapping or scattering cross section, we have

$$\frac{1}{\lambda_1} = \sqrt{2}\pi d^2 n(T) \tag{9}$$

where πd^2 is the trapping cross section. In the electrostatic trapping case, scheme II, we have

$$d = \frac{e^2}{8\pi\varepsilon_0\varepsilon_\infty k_B T} \tag{10}$$

which has been derived by equating the centripetal force of the moving cation in the vicinity of an anion trap with the Coulombic force of attraction between the anion and cation. As is customary in describing scattering processes, d is taken to be the effective diameter of the Coulombic potential of the mobile cation and the stationary anion. In this way d is also the effective radius of the trapping cross section.

Of the parameters in equation (10), all are well known except the limiting high-frequency optical dielectric constant ε_∞. Unfortunately, ε_∞ is not well known at this time for the silver thioborosilicate glasses because we can only measure up to 1 MHz on our impedance analyser and even at liquid nitrogen temperatures, because the conductivity of these glasses is so high, the contribution of the mobile ions to the measured dielectric constant is still strong. However, if we use the most probable thermal velocity calculated from equation (6), which will determine the interaction of a cation with traps, and an average cation separation distance from neutron scattering of ∼3 Å [20], a time scale for ionic interaction $\tau \sim 3$ Å$/200$ m s$^{-1} \sim 1.5 \times 10^{-12}$ s is estimated. For these reasons, we use the Lorentz–Mossotti relation $\varepsilon_\infty \sim n_0^2$ to determine ε_∞ where n_0 is the index of refraction.

It is noted that without an intrinsic LT limiting trap distance, λ_0, equation (8) predicts that the trap distance would increase at LTs to the unphysical value of infinity. Hence λ_0 essentially ensures the physically realistic situation that there will always be some longest trap distance in the glass. As a first approximation to this intrinsic trap distance, we will in scheme II take its value to be the separation distance determined by the carrier concentration at the glass transition temperature T_g. That is to say, at T_g there will be some fraction of thermally activated mobile carriers, determined by a Gaussian distribution of barrier heights, which leads to some 'frozen-in' limiting separation between cations. We believe this to be the shortest distance that the cations can migrate without incurring a trapping site and calculate λ_0 using

$$\lambda_0 = [n(T_g)]^{-1/3}. \tag{11}$$

Lastly we will assume that the activation energy barriers in these glasses, as is well-known and discussed [18, 21–26], are distributed such that equation (2) can be rewritten as

$$n(T) = \sum_i n_i \mathrm{e}^{-\frac{\Delta E_i}{k_B T}} \tag{12}$$

where n_i is the number density of cations residing in wells with an energy barrier ΔE_i and i spans the glass structure and includes all possible cation sites in the glass. For a Gaussian distribution of ΔE_i activation energies it can be shown exactly that equation (12) simplifies to

$$n(T) = n_{tot} \exp\left(-\frac{\overline{\Delta E_{act}}}{k_B T} + \frac{s^2}{2(k_B T)^2}\right)\frac{1}{2}\,\mathrm{erfc}\left(\frac{s}{\sqrt{2}k_B T} - \frac{\overline{\Delta E_{act}}}{\sqrt{2}s}\right) \tag{13}$$

where erfc is the error function, $\overline{\Delta E_{act}}$ is the average energy barrier for the distribution and s is the population standard deviation of the distribution. Hence, our final equation for the conductivity using these relationships becomes

$$\sigma_{dc}(T) = \frac{1}{2}\frac{\mathrm{e}^2 n(T)}{\sqrt{2mk_B T/3}}(\lambda_0^{-1} + \sqrt{2}\pi d^2 n(T))^{-1}. \tag{14}$$

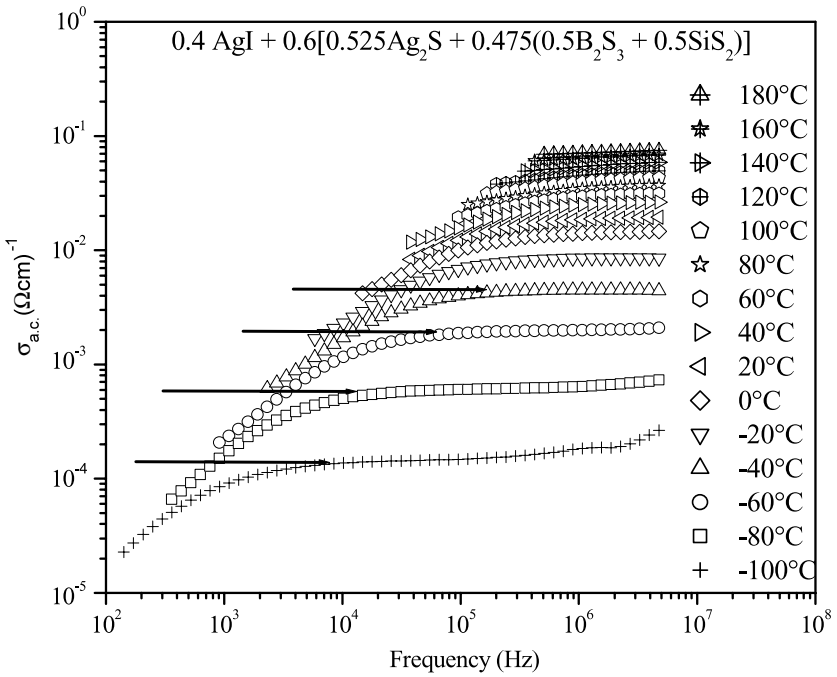

Figure 1. Plot showing the frequency dependence of the real part of the conductivity for glassy $0.4AgI + 0.6[0.525\ Ag_2S + 0.475(0.5\ B_2S_3 + 0.5SiS_2)]$ at different temperatures. The low-frequency polarization data have been removed from this plot to facilitate easier reading. Horizontal arrows show approximate values for the dc conductivity as determined by the 'plateau' value of the frequency-dependent conductivity.

The temperature-dependent concentration of mobile carriers, $n(T)$, is taken from equation (13). In the following, we will fit equation (14) to the dc conductivity reported in figure 1 for the silver thioborosilicate glasses. We will do this using the two schemes for the trapping mechanism described above. We will first (scheme I) fit this equation to the conductivity data leaving d as an adjustable parameter, the lattice gas scattering cross section diameter. In the second ionic lattice plasma treatment (scheme II), d will be calculated according to equation (10) using the index of refraction n_0 as the only adjustable parameter. In all of this, we will show that the fit to the experimental data is quite good for all compositions and temperatures and that all parameters take on physically reasonable values for silver thioborosilicate glasses. For example, the index of refraction values are constrained to a range expected for such glasses and are of the order $\sim$2. Also, the mean activation energy for the distribution is not arbitrarily adjustable as it must describe the LT-limiting Arrhenius region of the conductivity

3. Experimental details

3.1. Sample preparation

The starting materials AgI, Ag_2S and SiS_2 used to prepare the zAgI + $(1 - z)[0.525Ag_2S + 0.475(0.5B_2S_3 + 0.5SiS_2)]$ FIC glasses are commercially available in pure form. B_2S_3 is not, however, commercially available and was prepared in our laboratory by the stoichiometric reaction of boron and sulfur powder in an evacuated, carbon-coated silica ampoule [27].

All FIC glasses were prepared in an oxygen- and water-free (<1 ppm O_2, <1 ppm H_2O) glove box from stoichiometric amounts of AgI (Cerac, Inc. 99.999%), Ag_2S (Cerac, Inc. 99.9%), B_2S_3 and SiS_2 (Cerac, Inc. 99.5%). Appropriate amounts of these powders were weighed into a vitreous carbon crucible and were heated at 850 °C for 10 min. The samples were then checked for weight loss and reheated for an additional 5 min. Weight losses were checked and were always less than 1%. The liquid was poured into a brass mould at the anneal temperature, $T_g - 50$ °C, allowed to anneal for 30 min and then cooled at 5 °C min^{-1} to room temperature. The glasses were carefully annealed so that this process would not occur at elevated temperatures and in so doing be a possible source of the non-Arrhenius conductivity.

3.2. Impedance spectroscopy

Impedance spectroscopy using a Solartron 1260 impedance/gain phase analyser was used to determine the dc conductivity of these glasses. A frequency range of 0.01 Hz to 10 MHz was used with an amplitude of 0.05 V. A time delay of 2 s between data points and a 2 s integration time were also used to improve the accuracy of the data. Temperature control within the desired temperature range of −190 to 500 °C was ±1 °C.

4. Results

4.1. Experimental data

Figure 1 shows the real part of the conductivity as a function of frequency and temperature for the $0.4AgI + 0.6[0.525Ag_2S + 0.475(0.5B_2S_3 + 0.5SiS_2)]$ glass and reveals that the dc conductivity, approximately indicted on the curves as an arrow, increases as temperature is increased. A representative impedance plane plot used to determine the dc conductivity more accurately in the presence of electrode polarization processes for the $0.4AgI + 0.6[0.525Ag_2S + 0.475(0.5B_2S_3 + 0.5SiS_2)]$ glass is shown in figure 2. The arcs at high frequency represent the bulk response of the glass to an applied ac electric field and by determining where the arc intersects with the Z' axis, as shown by an arrow on a few of the arcs, the dc conductivity can be accurately determined. The beginning of a second arc can be seen at lower frequencies, which is believed to be due to polarization effects at the electrodes. As the temperature increases, the conductivity also increases and the more difficult it becomes to accurately determine the dc conductivity. Figure 3 shows the results for the dc conductivity so determined for all samples at all temperatures. The solid curves through the data points are guides to the eye and help to show the strong non-Arrhenius behaviour of the conductivity at high temperatures. The broken straight lines are best fits using an Arrhenius expression for the conductivity and are used to determine the LT average activation energy for the conduction process, $\overline{\Delta E_{act}^{Arr}}$ (see table 1). As the amount of AgI is increased, so is the deviation from Arrhenius behaviour, as illustrated in figure 3.

4.2. Fits to the data

Figures 4(A) and (B) show the fits of equation (14) to the conductivity data for the glasses with $z = 0.3$ and 0.4 respectively, using scheme I where λ_0 and d are taken to be independent (fitted) parameters. Table 1 shows the values of these parameters found from the fits. It is noticed that while λ_0 is of the order of the atomic spacing, ∼3–5 Å, the d values are relatively large, of the order of 50–100 Å. The activation energies, $\overline{\Delta E_{act}}$, are similar to those taken from the LT Arrhenius region of the dc conductivity, $\overline{\Delta E_{act}^{Arr}}$. The fit to the experimental data is good and the non-Arrhenius behaviour at elevated temperature is reasonably well reproduced.

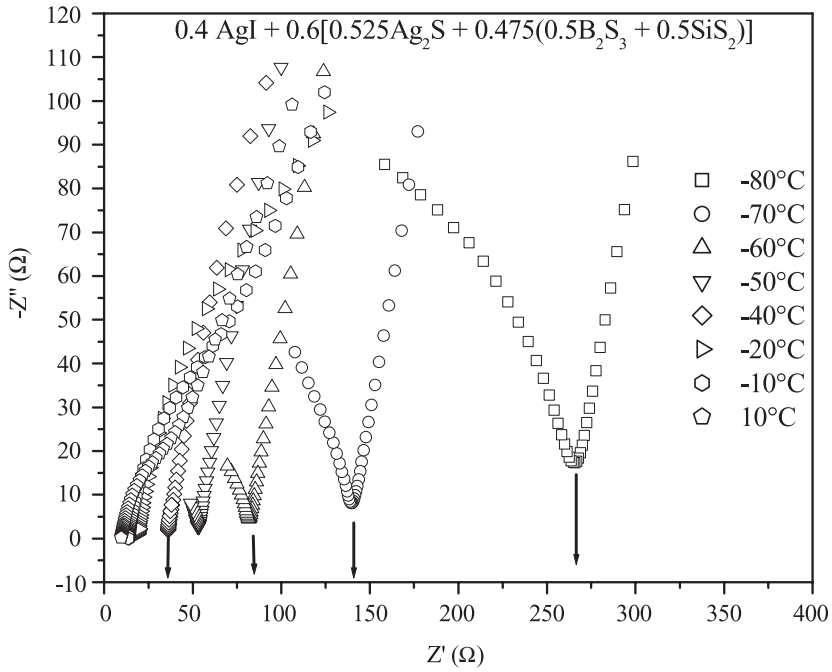

Figure 2. Impedance plane plots for the glass $0.4AgI + 0.6[0.525\ Ag_2S + 0.475(0.5\ B_2S_3 + 0.5SiS_2)]$ at a variety of temperatures illustrating the method used to determine the dc conductivity. Vertical arrows show how the dc impedance was determined from the minimum point on each curve. For the higher-temperature curves, where the equivalent circuit electrical relaxation frequency is beyond the limit of our impedance analyser, the dc impedance was determined by extrapolating the curve to the real impedance axis.

Table 1. Summary of the parameters used to fit the conductivity data for the zAgI + $(1 - z)[0.525Ag_2S + 0.475(0.5B_2S_3 + 0.5SiS_2)]$ glasses using scheme I where λ_0 and d are treated as completely adjustable (fitted) parameters. The average activation energies, $\overline{\Delta E_{act}^{Arr}}$, obtained from the Arrhenius fits to the LT conductivity data, are also given.

z	$T_g(\pm 2)$(K)	$\overline{\Delta E_{act}^{Arr}}(\pm 0.1)$ (kJ mol^{-1}) (LT region)	$\overline{\Delta E_{act}}(\pm 0.1)$ (kJ mol^{-1})	$\lambda_0(\pm 1)$ (Å) (fitted)	$d(\pm 10)$ (Å) (fitted)
0.0	631	27.11	27.44	19	100
0.1	561	27.50	25.77	10	20
0.2	542	24.22	25.77	6	100
0.3	525	20.94	20.04	2.1	65
0.4	528	19.97	18.29	5	30

Figures 5(A) and (B) show the fits of equation (14) to the conductivity data for the glasses with $z = 0.3$ and 0.4 using scheme II where λ_0 and d are calculated according to equations (11) and (10), respectively. Here λ_0 is taken to be an intrinsic trapping site distance frozen in at T_g and is calculated from the number of thermally activated cations at this temperature. The parameter d is calculated as the trapping distance (effective diameter) for a Coulombic trap of unit anion charge embedded in a medium of dielectric constant $\varepsilon_\infty \sim n_0^2$. We use adjustable values of n_0, between 1.5 and 2.5, which are considered to be representative of

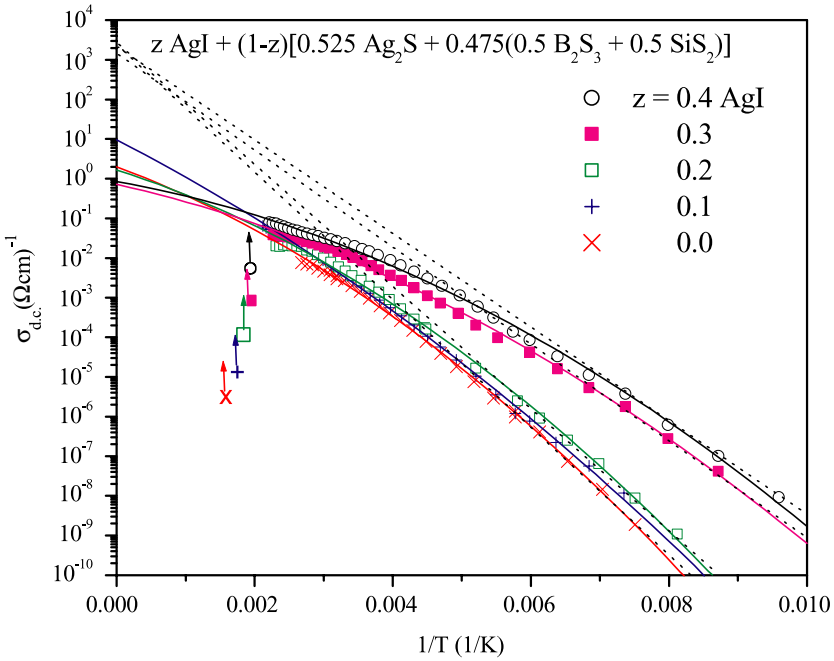

Figure 3. Plot of the temperature dependence of the dc conductivity for samples of composition zAgI + $(1-z)$[0.525 Ag_2S + 0.475(0.5 B_2S_3 + 0.5 SiS_2)]. The solid curves through the data are guides to the eye. The broken straight lines through the data are the extrapolations from LTs of Arrhenius fits, used to determine the average activation energy for the conductivity, $\overline{\Delta E_{act}^{Arr}}$, and show the level of deviation of the conductivity data away from Arrhenius behaviour at higher temperatures. The T_g values for the glasses, also given in tables 1 and 2, are shown by vertical arrows marked with a suitable symbol below the curve for each data set.

Table 2. Summary of the parameters used to fit the conductivity data for the zAgI + $(1-z)$[0.525Ag_2S + 0.475(0.5B_2S_3 + 0.5SiS_2)] glasses using scheme II where λ_0 was fixed according to equation (11) and n_0 was varied to give $\varepsilon_\infty \approx n_0^2$ (via the Lorentz–Mossotti relation) and hence d via equation (10). In this scheme n_0 was restrained to lie within the range of physically acceptable values for these glasses, i.e. between 1.5 and 2.5.

z	$T_g(\pm 2)$ (K)	$\overline{\Delta E_{act}}(\pm 0.1)$ (kJ mol^{-1})	$s(\pm 0.2)$ (kJmol^{-1})	$\lambda_0(\pm 1)$ (Å) (fixed at T_g)	$n_0(\pm 0.1)$ (fitted)
0.0	631	28.68	1.4	24.2	1.5
0.1	561	28.27	1.4	29.3	2
0.2	542	27.85	1.4	30.5	1.8
0.3	525	24.53	1.2	24.3	2
0.4	528	21.20	1.1	19.6	2.3

silver thioborosilicate glasses, and the parameters for scheme II are summarized in table 2. The Coulomb force acts over a range determined by the dielectric constant of the glass and the charge state of the anion trap. Smaller dielectric constant glasses with highly charged anions should exhibit larger trap diameters than those with a larger dielectric constant and smaller (unit) charged anions. The velocity of a cation will also affect the effective Coulombic trap distance. As indicated by equation (10), slower-moving cations at lower temperatures will be affected at larger distances than faster-moving cations at higher temperatures, i.e. the Coulombic trap distance (diameter) has an inverse temperature dependence.

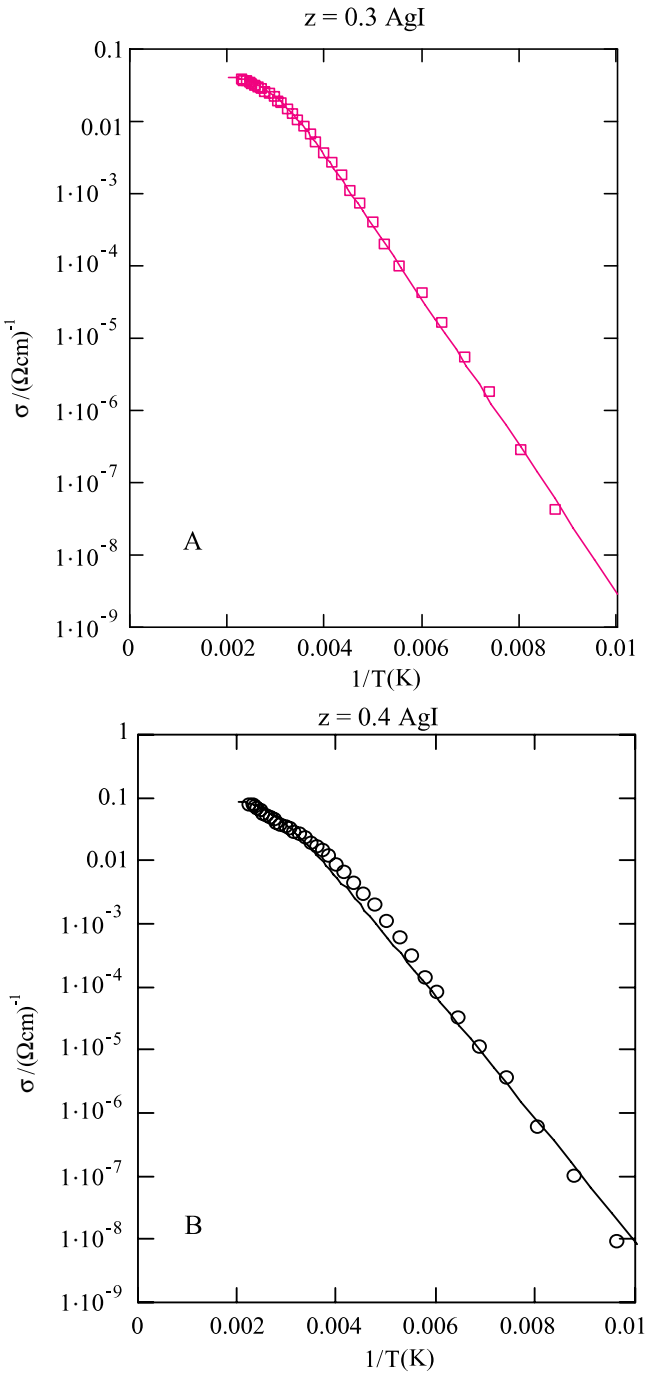

Figure 4. Fit of the conductivity data for the glass with $z = 0.3$ (A) or $z = 0.4$ (B) using scheme I of the trapping model (see the text). The best-fit values for λ_0 and d are given in table 1.

Figures 6(A) and (B) show the composition dependence of the average activation energy, $\overline{\Delta E_{act}}$, and index of refraction, n_0, respectively, used in scheme II. The index of refraction

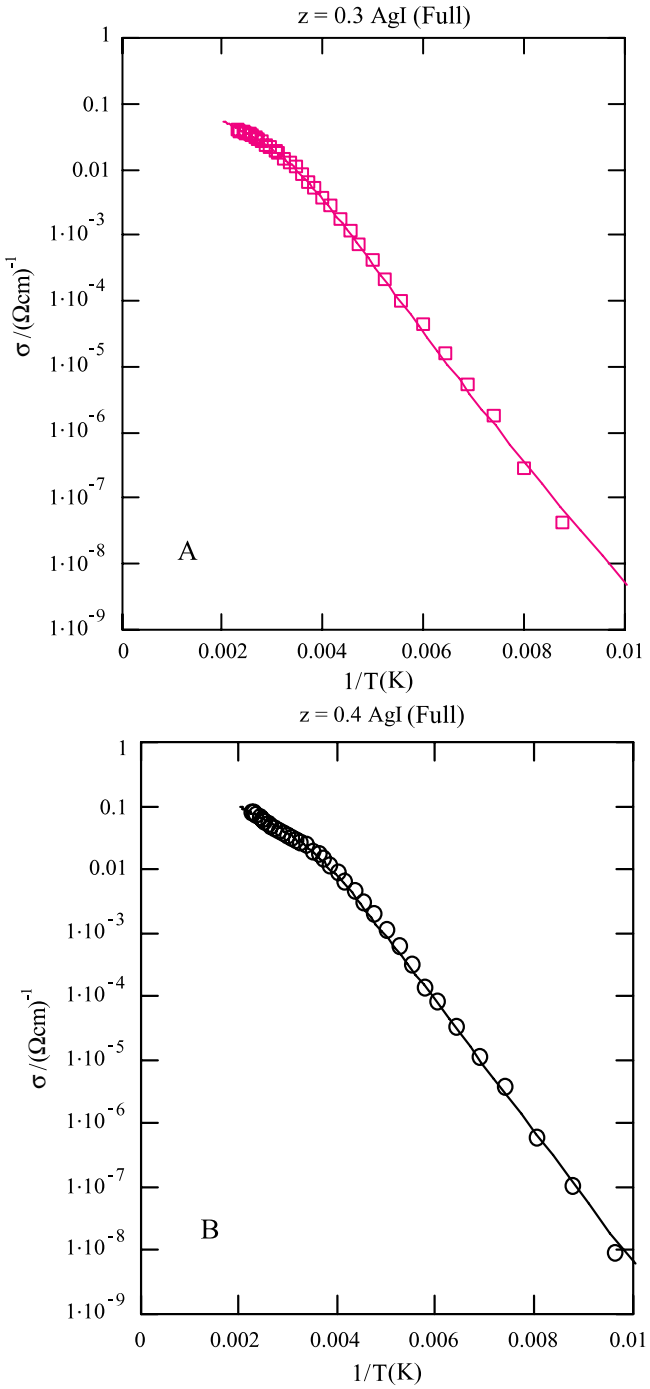

Figure 5. Fit of the conductivity data for the glass with $z = 0.3$ (A) or $z = 0.4$ (B) using scheme II of the trapping model. In this scheme λ_0 is calculated by using the value of $n(T)$ at T_g (equation (11)) and d is calculated according to equation (10) for a Coulombic trap embedded in a dielectric medium with dielectric constant ε_∞ (see the text). The index of refractive values, n_0, used to evaluate ε_∞ and hence d are given in table 2 together with the other relevant parameters.

values track very well the expected behaviour, increasing from a typical value of 1.5 for the undoped glass up to 2.3 for the highest-doped glass. While these values are obtained from fits to the data, they are also reasonable values for silver thioborosilicate glasses, i.e. significantly larger or smaller values than these would be unphysical. The best-fit values for the activation energies likewise track sensible values as shown by their comparison with the LT Arrhenius activation energies shown in figure 6(A).

Finally, figure 7 shows the conductivity data for all the glasses with best fits to equation (14) using scheme II denoted by full curves. The parameters used in equation (14) to fit the data are summarized in table 2. The fits to all of the conductivity data are quite good and all the parameters used in the modelling take on physically reasonable values.

5. Discussion

Figures 4, 5 and 7 show that the model developed in this paper is able to fit all of the data over all of the temperatures ranges with a high quality of fit. Both the LT Arrhenius and high-temperature non-Arrhenius regions are equally well represented, but the inclusion of the temperature-dependent Coulombic trap distance of scheme II, as given by equation (10), is shown to improve the quality of the fit. Indeed, the underlying physics of the Coulombic trap is likewise a more appealing model for a trap compared with an ideal gas scattering cross section as given by equation (9).

The basis of the model developed here is that the cations reside in Coulomb wells determined by the collective attractive potentials of nearby anions. In the silver thioborosilicate glasses these are the sulfide and iodide anions. Through thermal excitation, the cations are activated out of these sites and then migrate to other sites through random motions. These motions necessarily require the cations to migrate through the available interstitial free volume of the glass. Hence, the conductivity of these glasses is high for a number of reasons. First, the trapping potential of the anion sites in these glasses is low through the systematic use of weak-basicity sulfide and iodide anions. Second, the number of cations available for conduction has been made as high as possible through the use of large fractions of Ag_2S and AgI. Third, the migration pathways through the interstitial free volume of these glasses are made easier through the use of polarizable Ag^+ cations migrating through a structure of polarizable anions whose bonding is relatively weak. This relatively weak bonding, compared with more refractory oxide glasses, creates a glass structure that has a smaller mechanical modulus and as such is more susceptible to the dilation required as the cations migrate through the glassy network [28–31]. Therefore, the conductivity of these glasses, like that of all other glasses, increases with increasing temperature through the thermal excitation of mobile carriers.

The perhaps unique feature of the silver thioborosilicate glasses is their exceptionally low thermal activation energy. This causes, at any one temperature, the number of mobile cations in the glass to be significantly higher than for other typical ion-conducting glasses. This in turn causes the number of open anion sites, i.e. sites left vacant due to cation excitation, to be substantially higher than for these other glasses. Hence, our view of these glasses is that because the cations are so mobile, the number of trapping sites is higher than for other ion-conducting glasses. This causes the trap distance, the separation between open available sites, to become shorter more rapidly than for other lower conductivity glasses. Thereby, at LTs, the cations migrate through an interstitial glass network having relatively few cation sites and λ_1 is long compared with the inter-cation separation distance. At higher temperatures, however, the interstitial network has a relatively larger number of anion sites and cation trapping events which limit further migration are viewed as a possible mechanism for the non-Arrhenius temperature dependence of the conductivity.

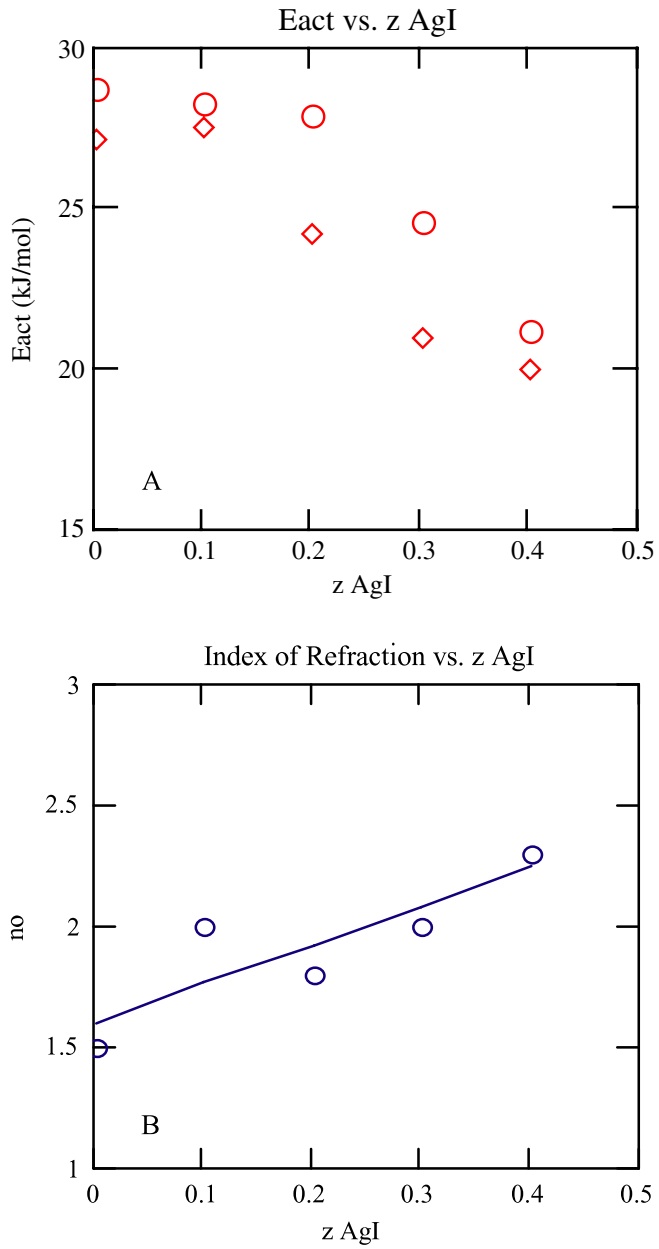

Figure 6. (A) Comparison of the composition dependence of the best-fit values for the average activation energy, $\overline{\Delta E_{act}}$, using scheme II (circles) and the LT Arrhenius activation energy, $\overline{\Delta E_{act}^{Arr}}$ (diamonds). Note the relative agreement in both the magnitude and composition dependence. (B) Composition dependence of the best-fit values for the index of refraction (circles). These values, while not experimentally determined, fall within an acceptable range as determined for other similar chalcogenide glasses. Note that the observed composition dependence is expected, i.e. the index of refraction increases with AgI content. The curve through the data is a best-fit straight line and is shown as a guide to the eye.

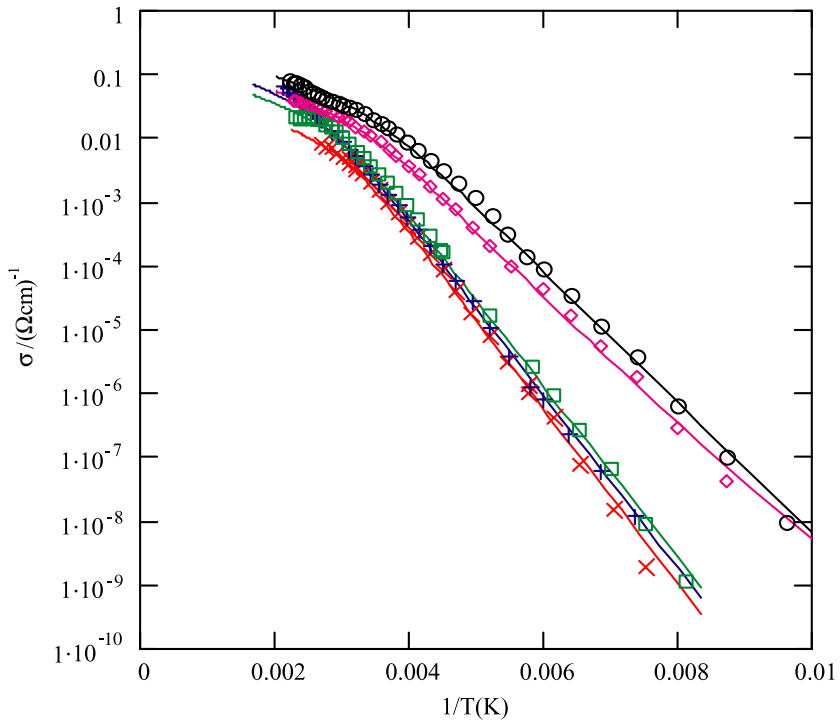

Figure 7. Experimental conductivity data for all of the glasses in the series zAgI + (1 − z)[0.525 Ag_2S + 0.475(0.5 B_2S_3 + 0.5 SiS_2)] and fits according to scheme II using the parameters given in table 2 (see the text).

In our scheme II representation of the non-Arrhenius conductivity there is only one truly adjustable parameter, i.e. the average activation energy $\overline{\Delta E_{act}}$, since the index of refraction is a measurable quantity. This activation energy is not, however, completely adjustable because the conductivity appears to return to Arrhenius behaviour at LTs and as such the model must also be capable of modelling this behaviour. The intrinsic jump distance λ_0 is likewise not completely adjustable. It is calculated through equation (11) in scheme II and as such it is fixed at the T_g of the glass. Finally, the index of refraction is also quite limited in its value and best fits were obtained when the physically reasonable values shown in figure 6(b) were used. The quality of fit, using such a restricted set of physically reasonable parameters in a particularly simple model, is indeed remarkable and strongly suggests that there may in fact be some merit to the concept of trapping-limited conductivity.

In the future, we will explore the veracity of this model by applying it to other glass-forming systems that exhibit both typical Arrhenius as well as atypical non-Arrhenius behaviour. Studies of both Ag^+ ion and Li^+ ion conductors are in progress and will be reported in the future. An important study also in progress is measurement of the optical range index of refraction for these glasses to see if the model predictions are as close as expected. Additionally, since the model predicts a strong dependence of the Coulomb trap distance on the index of refraction of the glass, we intend to examine a series of glasses whose carrier concentration, glass transition temperature, T_g, and other physical properties are closely matched, with the exception that their index of refraction and hence their optical frequency dielectric constant can be varied systematically. We will examine both Ag^+ and Li^+ ion conductors in this study.

6. Conclusions

An effective new model of ion conductivity for optimized FIC glasses has been developed. The essential feature of this model is that the mobile cations in these glasses conduct from an open available site to the next open available site. In this process, they naturally by-pass filled or unavailable sites. The thermal excitation of cations out of their equilibrium sites is taken to be the mechanism for generation of the open and available sites. Hence, the distance between trapping sites is a strong function of temperature. Two schemes for the trapping mechanism have been proposed for when a cation interacts with an open site. In the first and simplest scheme, we used simple ideal gas law scattering theory. This scheme, while reproducing the main features of the data, does not produce a strong enough temperature dependence for the conductivity. The second more physically appealing scheme is that of a Coulombic trap being created when a cation is thermally activated out of its site. The trap distance becomes temperature dependent through both the thermal creation of a site and also through the temperature-dependent drift velocity of the cations.

Scheme II is able to accurately reproduce the non-Arrhenius temperature dependence of the conductivity for the silver thioborosilicate series of chemically optimized FIC glasses. In this scheme there is in principle only one independent adjustable parameter, the average activation energy, and the scheme correctly accounts for both the magnitude and composition dependence of the index of refraction for these glasses. A limiting saturation value for the conductivity is predicted from the model to be in the range of $\sim 10^{-1}$–10^{0} Ω cm^{-1} at room temperature. This value arises from the competing effects of thermal creation of mobile carriers and the effective trapping of mobile carriers at short distances.

Acknowledgments

This work was supported by the National Science Foundation grant number DMR-9972466. SWM is grateful for the discussions of this model with Professors Borsa (ISU), Moynihan (RPI), Sidebottom (UNM), Maas (Konstanz) and Funke (Muenster).

References

[1] Funke K, Cramer C and Roling B 2000 Dynamics of mobile ions in glass—what do conductivity spectra tell us? *Glass Sci. Technol.* **73** 244
[2] Angell C A 1992 Mobile ions in amorphous solids *Annu. Rev. Phys. Chem.* **43** 693
[3] Fusco F A, Tuller H L and Button D P 1992 Lithium, sodium and potassium transport in fast ion conducting glasses: trends and models *Mater. Sci. Eng.* B **13** 157
[4] Pradel A and Ribes M 1992 Ionically conductive chalcogenide glasses *J. Solid State Chem.* **96** 247
[5] Martin S W 1991 Ionic conduction in phosphate glasses *J. Am. Ceram. Soc.* **74** 1767
[6] Ingram M D 1989 Ionic conductivity and glass structure *Phil. Mag.* B **60** 729–40
[7] Ingram M D 1987 Ionic conductivity in glass *Phys. Chem. Glasses* **28** 215
[8] Levasseur A *et al* 1981 Synthesis and electrical properties of new sulfide glasses with high ionic conductivity *C. R. Seances Acad. Sci.* II **293** 563–5
[9] Robert G, Malugani J P and Saida A 1981 Fast ionic silver and lithium conduction in glasses *Solid State Ion.* **3/4** 311
[10] Ravaine D 1980 Glasses as solid electrolytes *J. Non-Cryst. Solids* **38/39** 353
[11] Otto K 1966 Electrical conductivity of SiO_2–B_2O_3 glasses containing lithium or sodium *Phys. Chem. Glasses* **4** 29
[12] Kincs J and Martin S W 1996 Non-Arrhenius conductivity in glass: mobility and conductivity saturation effects *Phys. Rev. Lett.* **76** 70
[13] Schrooten J A 2001 Investigation into the non-Arrhenius behavior of fast ion conducting glasses *PhD Thesis* Iowa State University of Science and Technology

[14] Ingram M D, Vincent C A and Wandless A R 1982 Temperature dependence of ionic conductivity in glass: non-Arrhenius behavior in the silver iodide arsenate ($Ag_7I_4AsO_4$) system *J. Non-Cryst. Solids* **53** 73
[15] Maass P, Meyer M, Bunde A and Dieterich W 1996 Microscopic explanation of the non-Arrhenius conductivity in glassy fast ionic conductors *Phys. Rev. Lett.* **77** 1528
[16] Ngai K L and Rizos A K 1996 Parameterless explanation of the non-Arrhenius conductivity in glassy fast ionic conductors *Phys. Rev. Lett.* **76** 1296
[17] Martin S W 1991 Ionic conduction in phosphate glasses *J. Am. Ceram. Soc.* **74** 1767
[18] Kim K H, Torgeson D R, Borsa F, Cho J, Martin S W and Svare I 1996 Distribution of activation energies explains ionic motion in glassy fast ion conductors: 7Li NMR spin-lattice relaxation and ionic conductivity in $xLi_2S + (1 - x)GeS_2$ *Solid State Ion.* **91** 7
[19] Barrow G M 1979 *Physical Chemistry* (New York: McGraw-Hill)
[20] Matic A, Swenson J, Borjesson L, Longeville S, Lechner R E, Howells W S, Akai T and Martin S W 1999 Ionic motion of silver in super-ionic glasses *Physica* B **266** 69
[21] Svare I, Martin S W and Borsa F 2000 Stretched exponentials with T-dependent exponents from fixed distributions of energy barriers for relaxation times in fast-ion conductors *Phys. Rev.* B **61** 228
[22] Almond D P, Vainas B and Uvarov N F 1998 A new analysis of the bulk ac electrical response of ionic conductors *Solid State Ion.* **111** 253
[23] Isard J O 1996 High field conduction in ionic glasses-Effect of a distribution of activation energies *J. Non-Cryst. Solids* **202** 137
[24] Macdonald J R 1993 Distributed relaxation response for two classes of material temperature behavior *Phys. Status Solidi* b **176** 275
[25] Schirrmeister F, Kahnt H and Feltz A 1987 Frequency-dependent conductivity and the time distribution function of hopping events *J. Non-Cryst. Solids* **97/98** 523
[26] Martin S W, Borsa F and Svare I 1901 Distribution of activation energies treatment of fast ion motions in glass *Proc. Electrochem. Soc.* **2000-32** 66
[27] Martin S W and Bloyer D R 1990 Preparation of high-purity vitreous boron sulfide (B_2S_3) *J. Am. Ceram. Soc.* **73** 3481
[28] Swenson J, Matic A, Karlsson C, Borjesson L and Howells W S 2000 Free volume and dissociation effects in fast ion conducting glasses *J. Non-Cryst. Solids* **263/264** 73
[29] Fusco F A, Tuller H L and Button D P 1992 Lithium, sodium and potassium transport in fast ion conducting glasses: trends and models *Mater. Sci. Eng.* B **B13** 157
[30] McElfresh D K and Howitt D G 1986 Activation enthalpy for diffusion in glass *Comm. Am. Ceram. Soc.* **69** C-237–8
[31] Ryan M J and Smedley S I 1984 The effect of pressure on fast ion conductivity in glasses *J. Non-Cryst. Solids* **65** 29